VII - INTER-AMERICAN CONFERENCE ON MATERIAL TECHNOLOGY - OCTOBER/1981 - MÉXICO - MÉXICO

# ELECTRICAL RESISTIVITY MEASUREMENTS OF Nb-2,5 wt.%Zr ALLOY IN He ATMOSPHERE BEFORE AND DURING FAST NEUTRONS IRRADIATION.

M.P.Otero and G.Lucki

Instituto de Pesquisas Energéticas e Nucleares
São Paulo - Brasil.

ABSTRACT.

The solution behaviour of He in Nb-2,5wt.%Zr alloys was followed using electrical resistivity (ρ) measurements as a function of time (t) in polycristalline wires of commercial purity inclosed in He environment at a pressure of 1 kgf/cm$^2$ and at different temperatures (T) before and during neutron irradiation in order to simulate the conditions similar to the HTGR (High Temperature Gas Cooled Reactor).

From these measurements it is found out that the resistivity increases with the diffusion of He in the specimen at temperatures between 480 and 550°C the saturation being reached after 2 and 3 hours. Also, it was possible to determine parameters like relaxation time (τ), diffusion coefficients (D) and activation energy (E).

## I. INTRODUCTION.

Among many materials used in nuclear technology the Nb-Zr alloys can be put in evidence mainly in the fuel cladding (Zr-2,5%Nb), due essentially to the little cross section of neutrons absorption of both Zr and Nb and also in the internal lining of the walls in the reactor vessel because of the good corrosion resistance of the alloy[1].

The uses of this alloys will be extended in the future to the CTR - Controlled Termonuclear Reactor as components of the first wall.

In nuclear environments, as in the reactor core, the nuclear reaction $(n,\alpha)$ produces He atoms which can cause serious troubles to the reactors components, such as embrittlement (that appears in grain boundaries) and swelling. This swelling appears essentially through the vacancies supersaturation[2-4] and from the He bubbles[5-6]. In the case of Termonuclear Reactor, an integrated neutron flux between $10^{22}$ to $10^{23}$ n/cm$^2$,year is expected which will produce He at a rate in the range 10 and 200 ppm/year[7]. The purpose of the present paper is to study the He effect in the Nb-2,5 wt,%Zr alloy.

## II. EXPERIMENTAL PROCEDURES.

Everything that was said before consists of a fraction of the Radiation Damage. The Radiation Damage may be studied by means of various methods, among which, the most common are; the electrical[8], magnetic[9], mechanical and optical methods.

Practically all studies with the He gas effect in Nb and Nb-Zr alloys, consider the gas bubbles precipitation during the heat treatments with samples previously irradiated in a cyclotron, because high fluences in a reactor implie in a long time of irradiation[10-12]. Those experiments simulate the conditions that will appear in the futures reactors, such as HTGR, for example, where the enviroments are caracterized by high temperatures and He cooling. Although the helium solubility in metals is extremely small, Rimmer & Cottrell[5] showed that the He may be dissolved substitutionally when the vacancies are present. In this case one has a high vacancies concentration in thermal equilibrium due to the high temperature and neutron irradiation.

The present work is the study of the electrical properties ot the Nb-2,5 wt%Zr alloy, during irradiation (in situ) using an apropriate irradiation device with controlled temperature and atmosphere. The samples used in these experiments were prepared using Nb and Zr of 99,99% purity in an induction furnace with a vaccuum better than $10^{-5}$ torr. During irradiation these measurements were made using the irradiations facilities of the IPEN's reactor in a fast neutron flux of $5\times10^{12}$ n/cm$^2$,s (E > 1 MeV). For comparison sake the measurements were made also without irradiation. The method used was the standard 4 - wires and a DANA - 5800-A digital multimeter which incorporates an "Ohms Converter" module. The temperature was controlled by RT-3000- Setaram Electronic Temperature Controller which permits annealings with $\pm$ 1 $^{o}$C stability. The experiments were performed with samples as rolled, i.e., without initial heat treatment and with samples annealed at 1000 $^{o}$C during 1 h and cooled during 7 h in the furnace.

## III. RESULTS.

a) Isothermal annealings without irradiation.

Figure 1 shows a set of annealings made with samples of Nb-2,5wt.%Zr alloy that was previously molten in flowing Argon environment. The curves at temperatures of 511 $^{o}$C sample 1, 555$^{o}$C sample 2 and 555$^{o}$C sample 3,

show an increase of the electrical resistivity ρ with the time of annealing t. The curve that refers to sample 4 was obtained from an annealing at 555°C in vaccuum of $10^{-4}$ torr, A preliminary analysis suggests the existence of He dissolution in the sample when the annealing takes place in the He atmosphere at 1 kgf/cm$^2$ and, in the case of sample 4 there is an evidence of the occurrence of Argon release that was incorporated in the alloy during the melting, For this reason and also due to the occurrence of embrittlement of the samples further meltings were made in vaccuum,

The figures 2, 3 and 4 show the measurements taken in the following manner:

i) vaccuum: $10^{-2}$ torr at 500 °C sample 5; $10^{-4}$ torr at 600°C sample 5a; $10^{-5}$ torr without initial heat treatment samples 5b at 600°C, 5c at 650°C and 5d at 700°C;

ii) He atmosphere: 508°C sample 6, 602°C sample 7, 600°C sample 8, 600°C sample 8a, 700°C sample 8b and 650°C sample 8c; the following without initial heat treatment 8d at 600°C, 8e at 650°C and 8f at 700°C,

For samples 5, 5a, 5b, 5c and 5d, figs,2 and 4 no change in ρ was detected as it was expected,It is assumed that other processes are absent, such as ordering, phase precipitation etc., or if existent, have negligible contribution to ρ, In this case, one has $d\rho/dt = 0$, On the other hand, for samples 7,8,8a,8b and 8c, figs,2 and 4, ρ increases with time due to He gradually dissolved in the alloy, and for this case one has $d\rho/dt > 0$; the same considerations are valid for sample 6, fig,3. The difference between the behaviours of ρ in He atmosphere and in vaccuum, can be attributed to He, whose dissolution is facilitated by vacancies present at high temperatures, The difference in time of annealing in order to reach the saturation depends on various factors which are: initial heat treatment, thickness, temperature and He pressure, The thickness of the sample was set to be ~50 μm and the He pressure fixed at 1 Kgf/cm$^2$, The experiments were perfomed at various temperatures for samples without initial annealing as well as for samples with initial annealing. The curves 8a, 8b and 8c, fig,4, were obtained for samples with an initial heat treatment at 1000°C during 1 h and cooled during 7 h in vaccuum of $10^{-5}$ torr and the curves 8d, 8e and 8f for samples as rolled, i,e,, without initial heat treatment, A great influence of the initial heat treatment can be seen on fig, 4, The difference observed in the behaviour of ρ can be attributed to the following: samples 8d, 8e and 8f, as rolled, have a high concentration of defects such as, dislocations, vacancies etc., owing to the ~97% cold work, which permits the absorption of a high quantity of He, and consequently the rapid increase of ρ during the first h of annealing,

After 1 h, ρ has a small decrease and tends to the value for samples with initial heat treatment, because the defects of the cold work are annealed out and the excess of Helium atoms is released and the remaining He atoms migrate to reach a uniform distribution in the material, For samples 8a, 8b and 8c, the defect concentration of the cold work is very low, and the absorption of He atoms is very slow and takes place via grain boundaries and vacancies,

The difference in time of annealing in order to reach the saturation for samples 6 and 7, for example, can be attributed to the fact that:

$$C_{Tv}\ (600°C) > C_{Tv}\ (500°C) \qquad (1)$$

where: i) $C_{Tv}(T)$ = vacancies concentration in thermodynamic equilibrium at temperature T, Therefore it is ob-

mes $d\rho/dt = 0$, after 4 hours of annealing,

figure 2
figure 3
figure 4

b) Isothermal annealings during irradiation.

There is a special interest to know the behaviour of this alloys in nuclear environments, for this reason measurements during fast neutron irradiation were taken. The results are illustrated in figs.5 and 6 and, as it was expected, the irradiation enhanced diffusion and the He originated from $(n,\alpha)$ reaction lead the electrical resistivity to reach the saturation more rapidly than in the situation (a). Another factor that contributes to this fact is:

$$C_{Tv(irr.)}(608^{o}C) > C_{Tv(therm)}(602^{o}C) \quad (2)$$

where: i) $C_{Tv(irr.)}(608^{o}C)$ =vacancies concentration in thermodynamic equilibrium at 608°C during irradiation,
ii) $C_{Tv(therm.)}(602^{o}C)$ = vacancies concentration in thermodynamic equilibrium at 602°C without irradiation,

Figure 6 shows the curves of $\rho$ x t for measurements before and during irradiation allowing also a comparison between them. It was observed that during irradiation $d\rho/dt$ decreases more rapidly with the time of annealing than that without irradiation.

figure 5
figure 6

## IV. DISCUSSION.

Other informations may be taken from these data, such as: diffusion coefficients, relaxation time and activation energy of the predominant process in the alloy. This was done for samples with initial heat treatment where the predominant process is vacancies migration.

a) Relaxation time.

In order to determine the relaxation time, the ratio $\rho_o / \rho(t) \equiv n(t)$ was plotted on figures 7 and 8. These curves may be well described by:

$$n(t) = n_e + (n_o - n_e)\exp(-t/\tau) \quad (3)$$

where: i) $n_e = n(t)$ for $t \to \infty$, i.e., in the equilibrium state, when $d\rho/dt \to 0$;
ii) $\tau$ = relaxation time.

This relaxation time may be determined using the Nagy's method[12] which permits its evaluation from the following expression:

$$F(t) = \ln\{-[n(t) - n(t + \Delta t)]\} \quad (4)$$

for $\Delta t$ = 10 and 15 minutes ($\Delta t \ll 1$). Figure 9 illustrates this procedure.

figure 7
figure 8
figure 9

b) Activation Energy.

The activation energy $E^a$ may be determined assuming that the relaxation time follows the relationship of Arrhenius:

$$\tau = \tau_o \exp(E^a/kT) \quad (5)$$

Figure 10 shows the evaluation of the values $E_w^a$ = 1,16 eV and $E_w^a$ =0,99 eV of the activation energy without irradiation for two differents lots of samples, and $E_d^a$ = 0,93 eV, the activation energy during fast neutrons irradiation,

Rimmer[5] has evaluated the activation energy for He dissolution in Cu as been 2,5 eV when the dissolution takes place interstitially and 1,0 eV when substitutionally, Ullmaier[6] in his review paper shows calculations in which the formation energy for He in interstitials sites is very high ( ~ 4 eV) compared with that necessary to put it in vacancies sites ( 1 eV ) and that the migration energy for interstitial He is very low (~0,2eV) resulting from this, that all He atoms migrate to vacancies sites, i.e., to substitutional sites. In present work the more realistic, substitutional site model is adopted, but it is necessary to consider the He dissolution via grain boundaries since the samples are in polycristalline state. Helium Release experiments[14-15] in austenitic steels lead to calculations of 1 eV for the activation energy between 500 and 600°C which is in good aggreement with our result.

figure 10 - figure 11 - figure 12

c) Diffusion Coefficients,

The diffusion coefficients are given by[13]:

$$D = (a^2/24).1/\tau \qquad (6)$$

where: a = 3,29 Å = lattice parameter for Nb with ccc structure. Table I represents the values obtained for relaxation time, activation energy and diffusion coefficients.

TABLE I

| Experiment | Temperature T(°C) | Relaxation Time τ (min) | Diffusion Coeff. $D(10^{-21})$ $(cm^2/s)$ | Activation Energy $E^a$ (eV) |
|---|---|---|---|---|
| Without irradiation, | 600 | 100 | 7,5 | 0,99±0,09 |
| | 650 | 34 | 22,1 | |
| | 700 | 26 | 28,9 | |
| | 508 | 312 | 2,4 | 1,16±0,10 |
| | 600 | 60 | 12,6 | |
| | 602 | 42 | 17,9 | |
| During Irradiation, | 488 | 272 | 2,8 | 0,93±0,09 |
| | 542 | 247 | 3,1 | |
| | 608 | 40 | 18,8 | |

d) Vacancies Supersaturation,

As the vacancies concentration is inversely proportional to the relaxation time ($C_v \propto 1/\tau$), one defines the vacancies supersaturation to the relationship:

$$S = \tau_w/\tau_d \propto C_{vd}/C_{vw} \qquad (7)$$

where: i) $\tau_w$ =relaxation time for the annealings before irradiation,

ii) $\tau_d$ = relaxation time for the annealings during irradiation.

The value S is a quantitative expression of how many times the vacancies concentration present during irradiation is larger than that present without irradiation. It is a necessary condition to the cavity formation and for the swelling of the material.

tion curves for FeNi and FeNi with impurities, An introduction of a little quantity of Cr (0,1at,%) to FeNi alloy, improves the material characteristics because the vacancies supersaturation is reduced markedly, thus this alloy will be better to nuclear environments than the others, p,ex,, FeNiMo (50-50 at,%+50 ppm), The vacancies supersaturation curve for Nb-2,5wt,%Zr is given in the figure 12, and it can be seen that this material is more indicated for power reactors than those of the figure 11,

Table II compares the values of S determined by G,Lucki et Al,[4] for FeNi with impurities by means of MAE - Magnetic After Effect with that for Nb-2,5wt,%Zr by means of resistivity, for a temperature close to 490°C

TABLE II

| Alloy | T(°C) | S |
|---|---|---|
| FeNi(50-50at,%) | 490 | 39,90 |
| FeNiMo(50-50 at,%+ 50 ppm) | 480 | 162,12 |
| FeNiCr(49,95-49,95-0,1 at,%) | 490 | 51,00 |
| Nb - 2,5 wt,% Zr | 500±10 | 1,15 |

## V, CONCLUSIONS,

There is an evidence that He dissolution occurs in the Nb-2,5wt,%Zr alloy when the isothermal annealings are made at high temperature and He atmosphere, This He dissolution may be detected by means of electrical resistivity ρ, This process of He diffusion is followed by an efective interaction of the atoms with other defects, mainly with vacancies and vacancies clusters, and this interaction affects markedly the electrical resistivity, At temperature 600 °C, ρ increases until to reach the saturation , During fast neutron irradiation this saturation is reached more rapidly than those without irradiation, This isothermal annealings has permited to calculate the relaxation time (τ), diffusion coefficients (D) and activation energy $E^a$ for the defects of the lattice structure of the alloy with He impurity, mainly the vacancies, In order to obtain the migration energy of the He in the Nb-2,5wt, % Zr alloy, it will be necessary other experiments of ρ with and without irradiation in vaccuum and in He atmosphere at various temperatures, Also the He release of this alloy will be made with samples previously annealed in He atmosphere and with samples previously irradiated in the reactor core and with α particles in the cyclotron,

Another parameter estimated was the vacancies supersaturation S, The value obtained here S =1,15 for T = 500 °C closed to S = 1,0, the limit for $T \to T_m$ ($T_m$ ~2,400 °C), is very desirable for the alloys of nuclear designs, This value of S, which is lesser than those for FeNi and FeNi with impurities of Cr, Si and Mo, may be explained in terms of cross section σ for fast neutrons absorption, In the table III are given the σ for the principals elements that form the alloys cited above,

TABLE III

| Element | Nb | Zr | Fe | Ni | Cr | Si | Mo |
|---|---|---|---|---|---|---|---|
| Cross section σ (b) | 1,15 | 0,185 | 2,55 | 4,43 | 3,1 | 0,16 | 2,65 |

This permits the conclusion that Nb-Zr alloy, are more "transparents" to fast neutrons than the other alloys and the consequence of this is that the vacancies concentration during neutron irradiation defers very little from that without irradiation, So it is possible to choose the Nb-2,5wt,%Zr alloy as the material for nucle

as the fuel cladding due to low fast neutron absorption,

VI. REFERENCES.


(1) Bölsing, F. & Dressler,G. The Matellography of Zr and Nb Alloys, "Practical Metallography", v.6, pp. 706-710, 1967.

(2) Sciani, V. & Lucki, G., "Radiation Damage Studies in the Magnetic Properties of the FeNi Alloys", 3º CBECIMAT (Brasilian Meeting of Engineering and Materials Sciences pp.D11.1-D11.11, Rio de Janeiro, 1978.

(3) Camargo, M.U.C., "Radiation Damage Studies in the Austenitic Stainless Steel AISI 321 with Nb aditions, with Heat and Mechanical Treatments and with Fast Neutron Irradiations" (IPEN-M.Sc. Thesis), São Paulo,1979.

(4) Lucki, G.; Veissid, N.; Sciani, V.; Otero, M.P., "Vacancies Supersaturation in Metallic Alloys during Neutron Irradiation, as a Selection method of Nuclear Materials", XXXI - Annual Meeting of ABM (Brasilian Metallurgical Association), Belo Horizonte, 1976.

(5) Rimmer, D.E. & Cottrell, A.H., "The Solution of Inert Gas Atoms in Metals", Phil.Mag. v.2, pp.1345-52, 1957.

(6) Ullmaier, H. & Schilling, W., "Radiation Damage in Metallic Reactor Materials", Physics of Modern Materials, v.1, IAEA-SMR-46/105, pp.301-397, 1980.

(7) Sagues, A.A., & Auer, J., "Mechanical Behaviour of Nb-1%Zr Implanted with He at Various Temperatures", International Conference on "Radiation Effects and Tritium Technology for Fusion Reactors", Gatlinburg,Tenn, USA, 1975.

(8) Otero, M.P, & Lucki, G, "Study and Characterization of the Electrical Properties of the FeNi (50-50 at.%) and NiCr(80-20 wt.%) Alloys During Fast Neutron Irradiation",VI Inter-American Conference on Materials Technology, San Francisco, California,Aug.12 15, 1980.

(9) Lucki, G, "Effects of Fast Neutrons Irradiations in the Magnetic Properties of the FeNi Alloy with and without Si and Mo Impurities",(Doctor Graduation), São Paulo,1971

(10) Tyler, S.K. & Goodhew, P.J., "Irregular Helium Bubbles in Niobium Alloys",J.of Micr., v.116, pp. 55-63, 1978.

(11) Tyler, S.K. & Goodhew, P.J.,"The Growth of He Bubbles in Nb and Nb-1%Zr", J.Nucl.Mat. v.74,pp.27-33, 1978.

(12) Nagy, E.J. Phys.Chem.Solids, v.23, pp.1605, 1962.

(13) Wert, C. & Zerner, C.Phys.Rev.,v.7, pp.1169 -1175, 1949.

(14) Kislik V.S.J., J.Nucl.Mat., v.75, pp.201-208, 1978.

(15) Karasev, V.S.; Kislik, V.S.; Shved, G.F.; Grebennikov,R.V., Soviet Atomic Energy, v. 34, pp. 321-4, 1973.

Fig.1 - Isothermal annealings without irradiation, a-sample 2, as rolled, He atm., b-sample 1, as rolled He atm., c-sample 3, after initial heat treatment, He atm., d-sample 4, after initial heat treatment, vaccuum. All samples melted in Argon atmosphere.

Fig.2 - Isothermal annealings without irradiation. In He atmosphere: a-sample 7, b-sample 8. In vaccuum: d-sample 5 ($10^{-2}$ torr), e-sample 5a ($10^{-4}$ torr) The curve c, was calculated by the equation

$$\rho(t) = \rho_s + (\rho_o - \rho_s)\exp(-t/\tau),$$

Fig.3 - Isothermal annealing without irradiation, in He atmosphere.

Fig.4 - Isothermal annealings without irradiation. The effect of heat treatment on He dissolution. Samples 5b,5c,5d without initial heat treatment, Vaccuum. Samples 8a,8b,8c with initial annealing, He atm. Samples 8d,8e,8f without initial annealing, He atmosphere.

Fig.5 - Isothermal annealings during irradiation. He atm, a-sample 11, b-sample 10, c-sample 9.

Fig.6 - Isothermal annealings:
In He atm: a,c,d - without irradiation
b,e - during irradiation
In vaccuum: f, g - without irradiation

Fig.7 - Plot of $\rho_o / \rho$ x t without irradiation, (x) curve calculated by
$n(t) = 0{,}655+0{,}34\exp(-t/60)$.

Fig.8 - Plot of $\rho_o / \rho$ x t during irradiation, (x) curve calculated by
$n(t) = 0{,}693+0{,}307\exp(-t/44)$.

Fig.9 - Evaluation of the Relaxation Time by Nagy's method.

Fig.10 - Evaluation of the Activation Energy.

Fig.11 - Vacancies Supersaturation curves for FeNi with and without impurities.

Fig.12 - Vacancies Supersaturation curve for Nb-2,5wt.% Zr alloy.

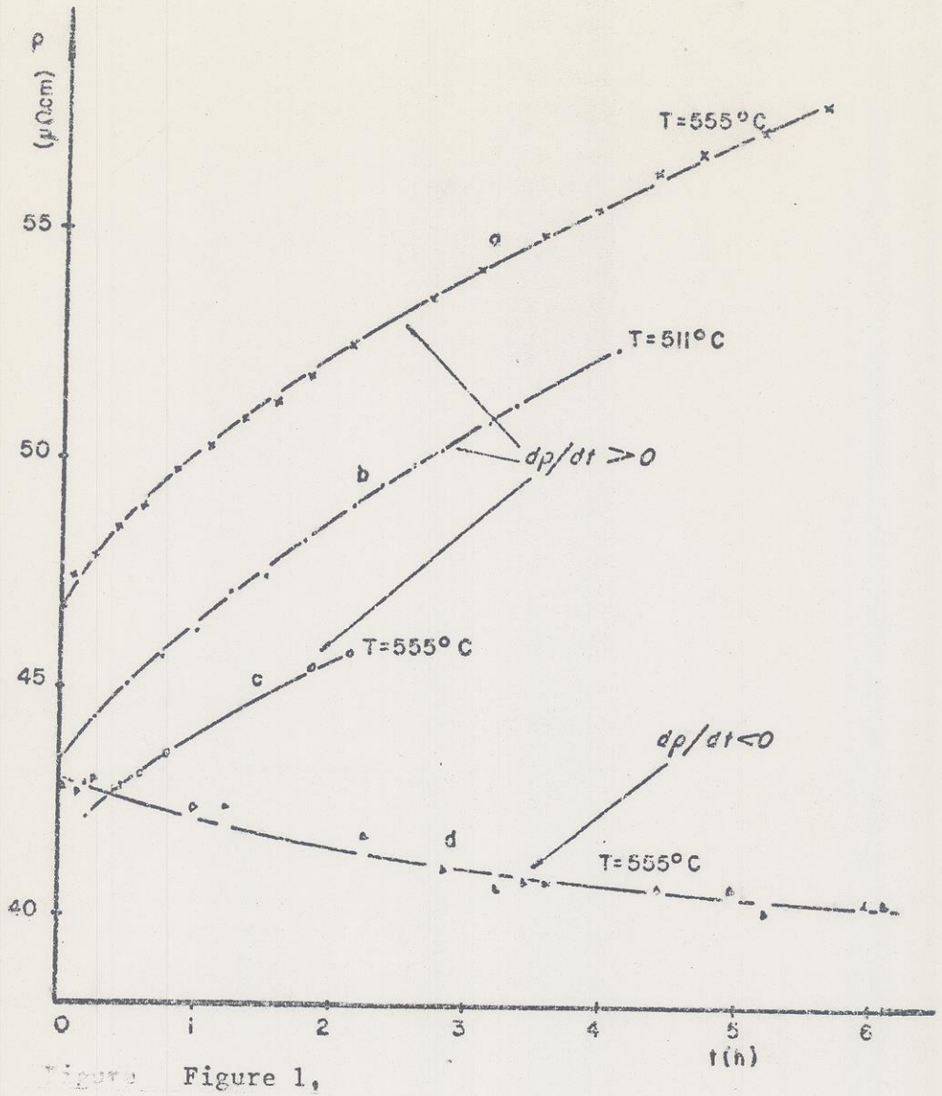


Figure 1,

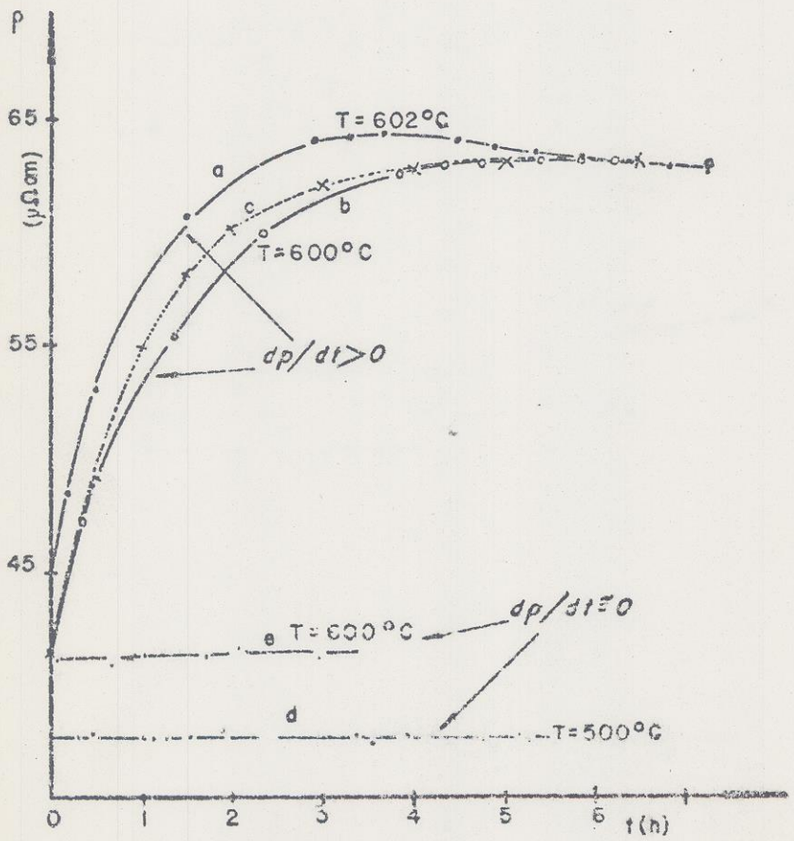


Figure 2

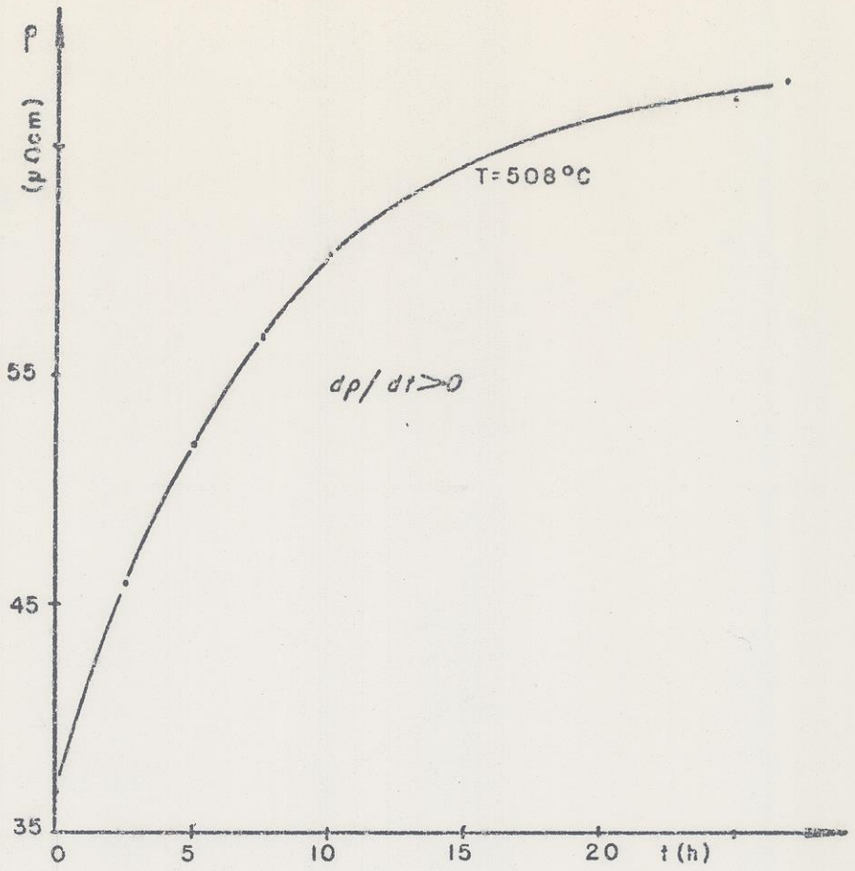


Figure 3

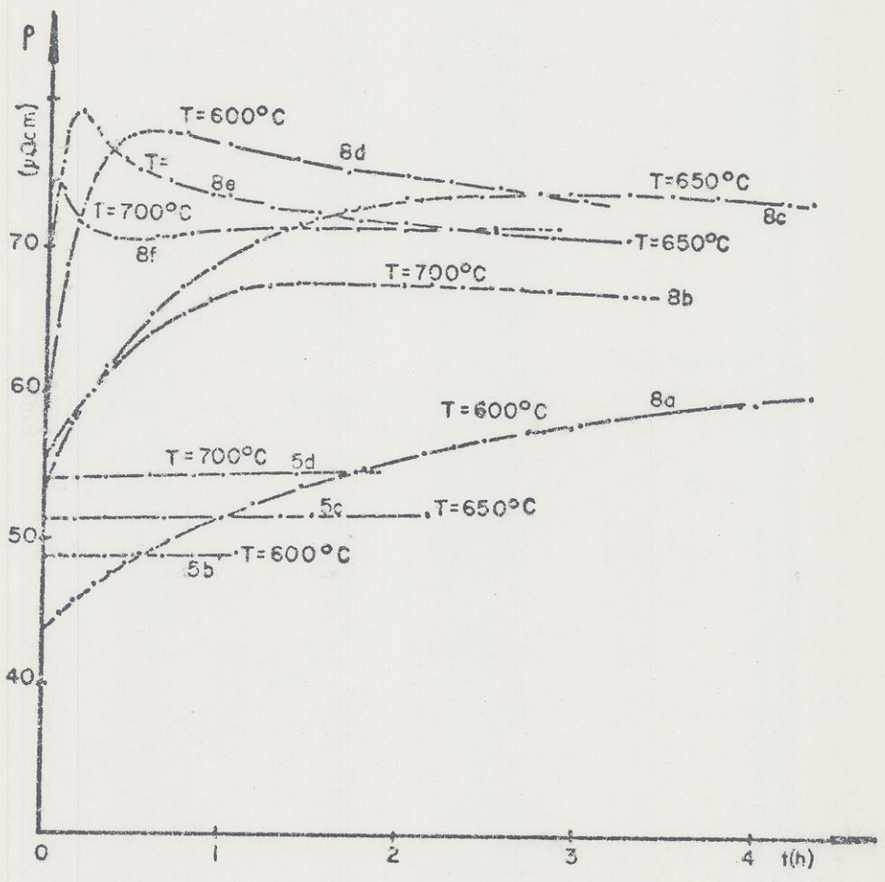


Figure 4

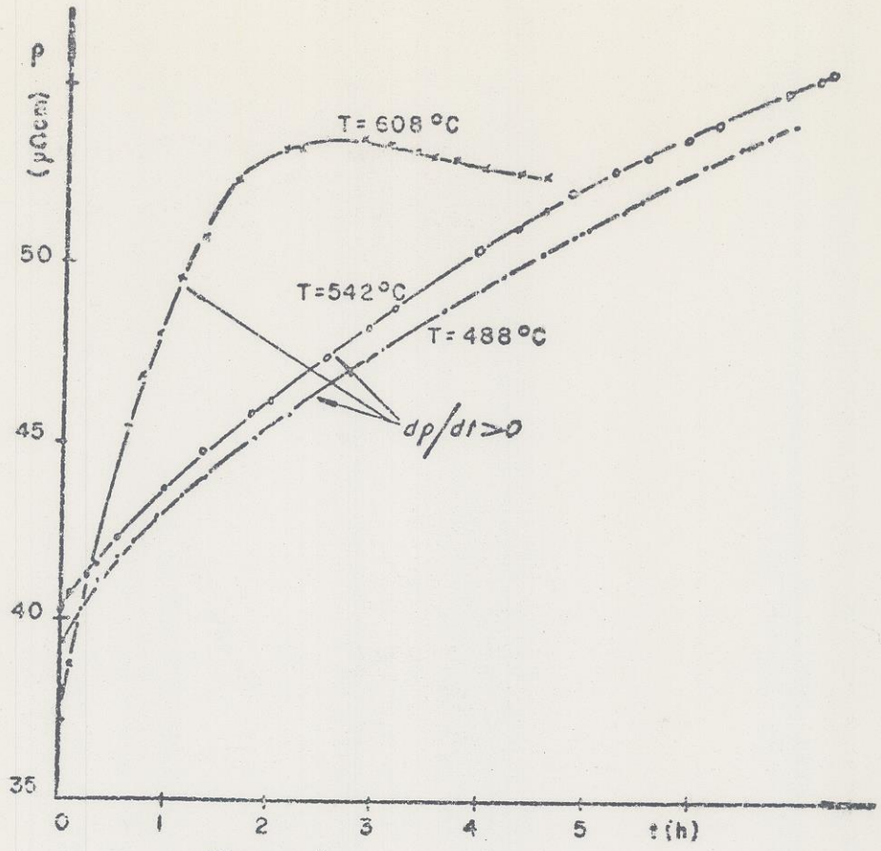


Figure 5

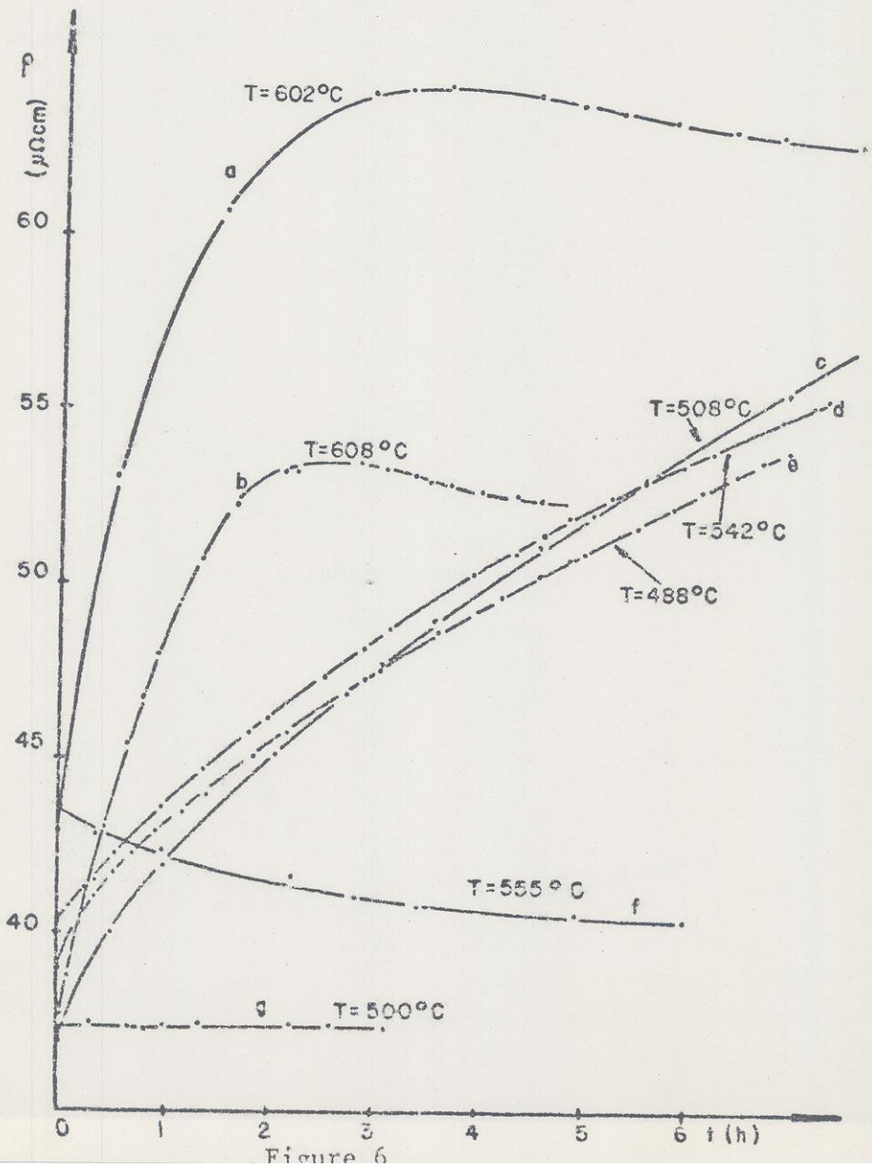


Figure 6

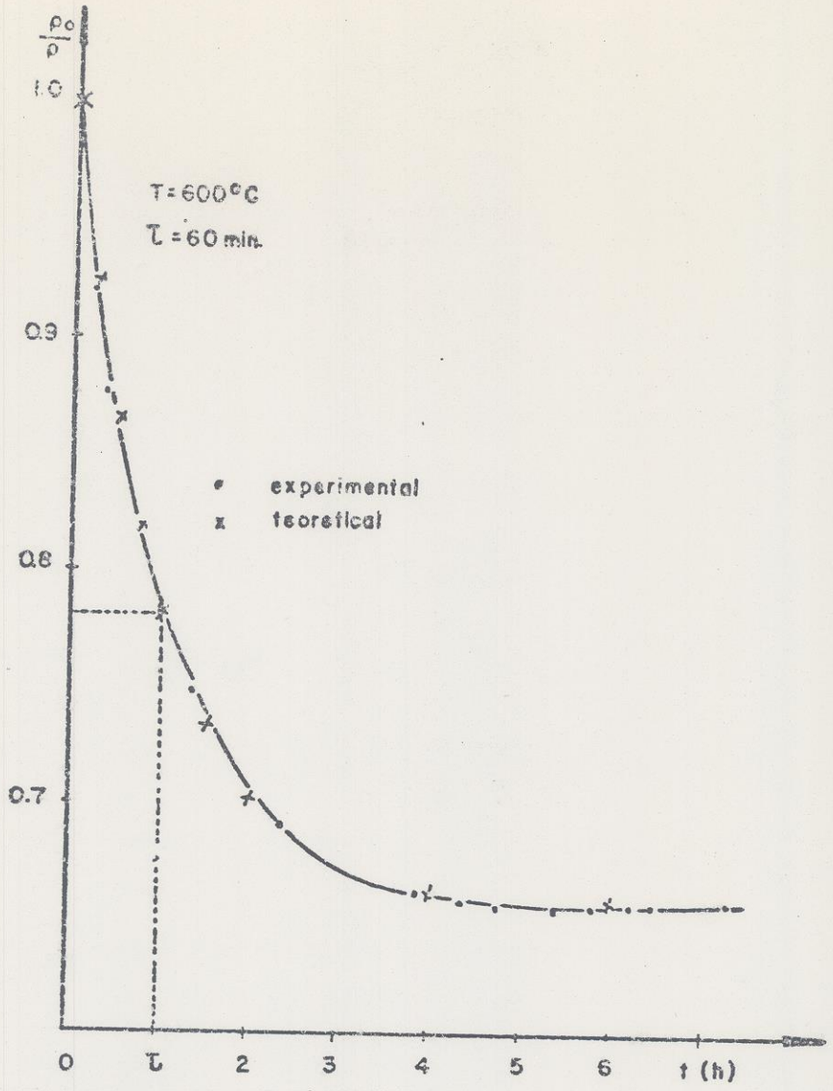
ρo/ρ
1.0
0.9
0.8
0.7
T=600°C
τ=60 min.
experimental
teoretical
0
τ
2
3
4
5
6
t (h)

Figure 7

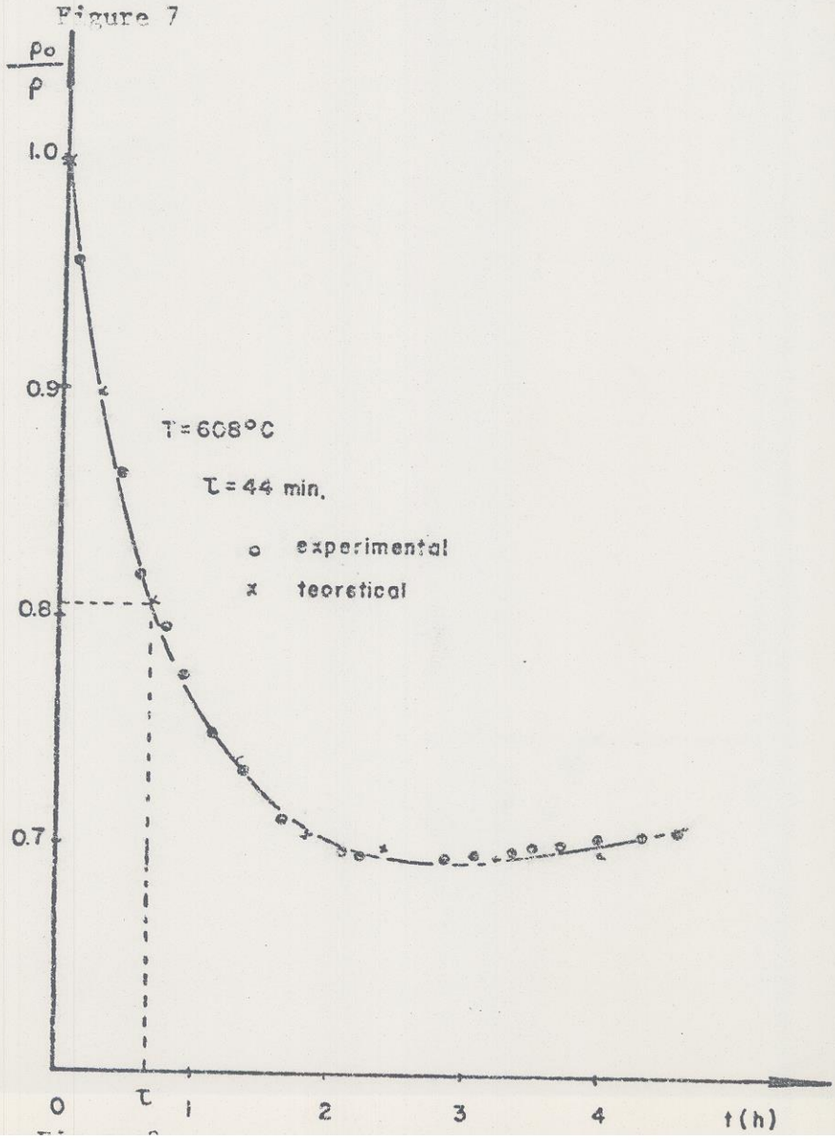
ρo/ρ
1.0
0.9
0.8
0.7
T=608°C
τ=44 min.
experimental
teoretical
0
τ
1
2
3
4
t (h)

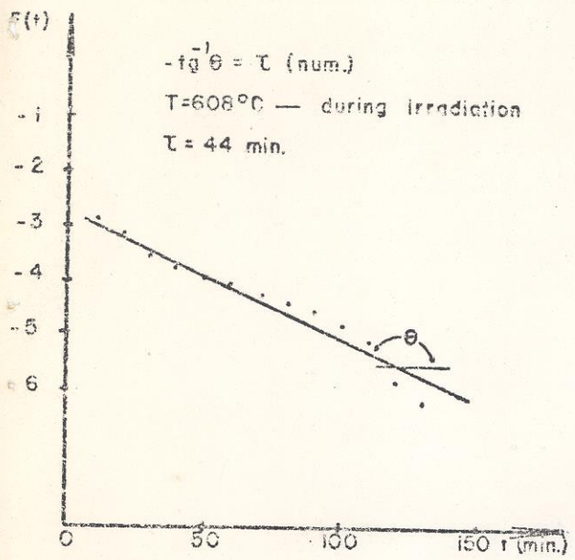


Figure 9

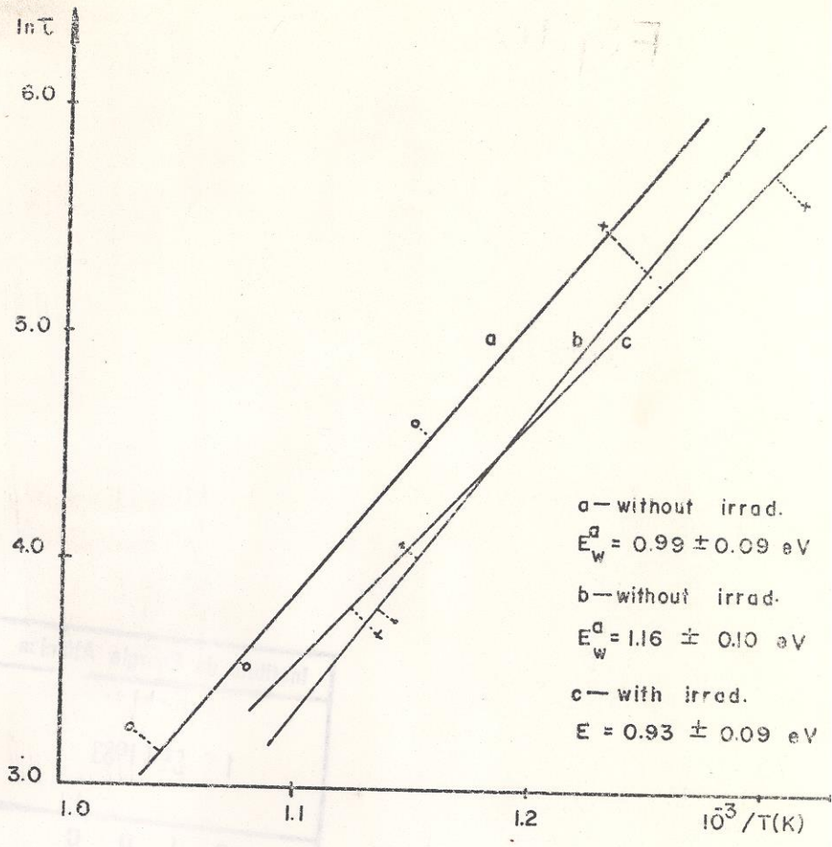


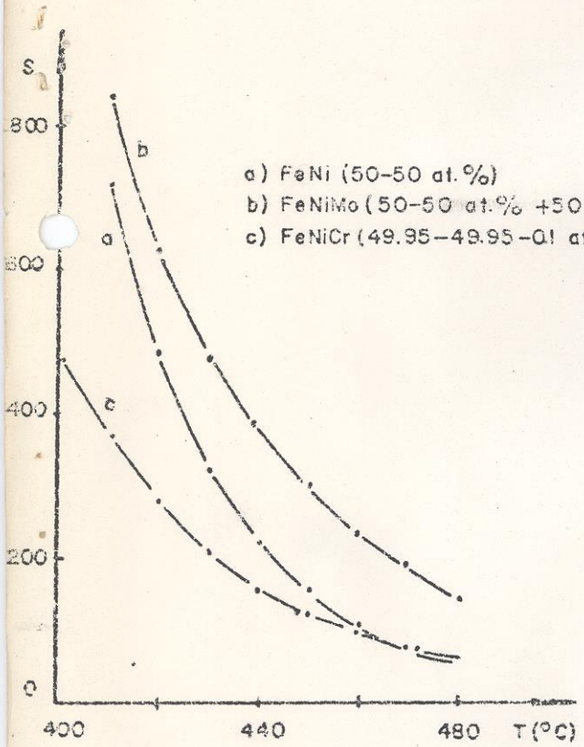


Figure 11

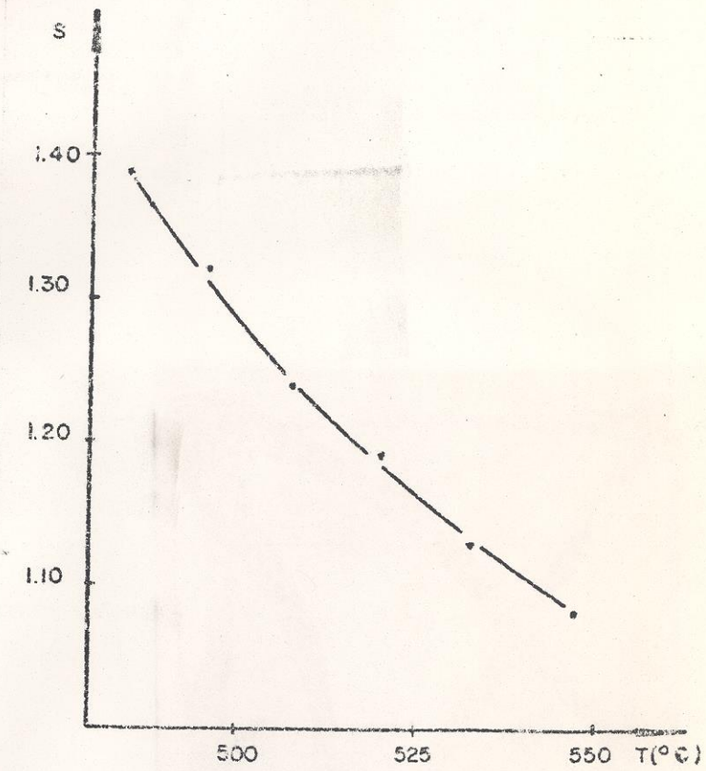


Figure 12